

## Supramolecular systems based on 1-alkyl-4-aza-1-azoniabicyclo[2.2.2]octane bromides

T. N. Pashirova, E. P. Zhil'tsova,\* R. R. Kashapov, S. S. Lukashenko, A. I. Litvinov, M. K. Kadirov, L. Ya. Zakharova, and A. I. Konovalov

A. E. Arbuzov Institute of Organic and Physical Chemistry, Kazan Scientific Center of the Russian Academy of Sciences, 8 ul. Akad. Arbuzova, 420088 Kazan, Russian Federation.

Fax: +7 (8 432) 73 2253. E-mail: Zhiltsova@iopc.knc.ru

The aggregation in aqueous solutions of alkylated 1,4-diazabicyclo[2.2.2]octanes of various hydrophobicity and their adsorption at the water–air interface were studied by tensiometry, conductometry, potentiometry, viscosimetry, and ESR spectroscopy. The parameters of adsorption, critical micelle concentrations, concentrations of free counterions (bromide ions), and degree of binding of the counterions with micelles were determined. The intensification of the micelle formation ability of the surfactants with an elongation of the alkyl fragment was shown. The effective radii of ensembles of the hexadecyl and octadecyl derivatives were determined by the dynamic light scattering method. A relationship between the concentration dependences of the size of micelles and their shape was established.

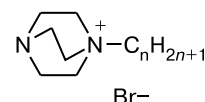
**Key words:** alkylated 1,4-diazabicyclo[2.2.2]octanes, adsorption, association, critical micelle concentration, ensemble radius, micelle shape.

1,4-Diazabicyclo[2.2.2]octane (DABCO) and its derivatives find wide use as efficient catalysts of the Baylis–Hillman<sup>1</sup> and Suzuki–Miyaura<sup>2</sup> reactions, in polyurethane synthesis,<sup>3</sup> for the induction of the Ramberg–Bäcklund rearrangement,<sup>4</sup> preparation of inhibitors of dioxycuanosine photooxidation,<sup>5</sup> photogeneration of free radicals of idebenone<sup>6</sup> and nitronaphthalenes,<sup>7</sup> and complexation with hydrogen peroxide<sup>8</sup> and calix[4]arenes.<sup>9,10,11</sup>

Among the known salt of DABCO structures are its nitrates and alkyl nitrates,<sup>12,13</sup> substituted DABCO with aldehyde,<sup>14</sup> benzyl,<sup>15</sup> and alkyl fragments.<sup>16,17</sup> Interest in the latter are due to their use as ionic liquids,<sup>18</sup> extracting agents of nucleoside phosphates,<sup>16</sup> and catalysts of hydrolysis of *p*-nitrophenyl diphenyl phosphate.<sup>14</sup> The dependence of the chemical effect on the hydrocarbon radical length was revealed for hydrophobized DABCO. For instance, in the conjugate of the bisquaternary salt of DABCO and imidazole, the substitution of the ethyl radical for tetradecyl resulted in a tenfold increase in the degree of cleaving of phosphorus diester bonds in RNA.<sup>19</sup> Although the role of hydrophobicity in the physicochemical properties of the DABCO compounds is very important, only few studies are devoted to this problem.<sup>14,19</sup> At the same time, the amphiphilic nature of alkylated DABCO makes it possible to classify them as surfactants, which are characterized by the ability to decrease surface tension in solutions due to adsorption and orientations of molecules at the interface and to form micelles at concentra-

tions above a certain concentration named the critical micelle concentration (CMC).<sup>20</sup>

In this work, we studied the aggregation in aqueous solutions of alkylated DABCO (AD) with different hydrophobicities (1–4) and the adsorption of these compounds at the water–air interface.



1–4

*n* = 12 (1), 14 (2), 16 (3), 18 (4)

Tensiometry, conductometry, potentiometry, dynamic light scattering, viscosimetry, and ESR spectroscopy were used as methods of investigation.

### Experimental

#### 1-Dodecyl-4-aza-1-azoniabicyclo[2.2.2]octane bromide (1).

A solution of dodecyl bromide (6.65 g, 0.0257 mol) in acetone (20 cm<sup>3</sup>) was added dropwise with stirring to a solution of 1,4-diazabicyclo[2.2.2]octane (3 g, 0.0267 mol) in acetone (20 cm<sup>3</sup>) cooled to 18 °C. The temperature of the reaction mixture was maintained at 18–20 °C. The resulting reaction mixture was stirred for 1 h at 20 °C and for 30 min at 45–50 °C. Solvent excess was distilled *in vacuo*. The salt precipitated was filtered off, recrystallized from acetone, and dried *in vacuo*. The product was obtained in a yield of 6.4 g (66%), m.p. 148–150 °C.

IR (KBr),  $\nu/\text{cm}^{-1}$ : 2920, 2849, 1469, 1377, 1098, 1057, 852, 796, 720.  $^1\text{H}$  NMR ( $\text{CDCl}_3$ ),  $\delta$ : 0.88 (t, 3 H,  $\text{CH}_3$ ,  $J = 6.8$  Hz); 1.32–1.35 (m, 18 H,  $\text{CH}_2\text{CH}_2(\text{CH}_2)_9\text{CH}_3$ ); 1.73–1.78 (m, 2 H,  $\text{CH}_2\text{CH}_2(\text{CH}_2)_9\text{CH}_3$ ); 3.27 (t, 6 H,  $\text{N}(\text{CH}_2\text{CH}_2)_3$ ,  $J = 7.3$  Hz); 3.46–3.53 (m, 2 H,  $\text{N}^+\text{CH}_2$ ); 3.68 (t, 6 H,  $\text{N}^+(\text{CH}_2\text{CH}_2)_3$ ,  $J = 7.3$  Hz). Found (%): C, 59.86; H, 10.24; Br, 22.15; N, 7.75.  $\text{C}_{18}\text{H}_{37}\text{BrN}_2$ . Calculated (%): C, 60.04; H, 10.52; Br, 21.11; N, 7.70.

Compounds **2–4** were synthesized according to a similar procedure with recrystallization from an acetone–methanol mixture. Their characterization is given below.

**1-Tetradecyl-4-aza-1-azoniabicyclo[2.2.2]octane bromide (2).** The yield was 72%, m.p. 166–168 °C. IR (KBr),  $\nu/\text{cm}^{-1}$ : 2918, 2848, 1470, 1376, 1095, 1057, 852, 795, 720.  $^1\text{H}$  NMR ( $\text{CDCl}_3$ ),  $\delta$ : 0.88 (t, 3 H,  $\text{CH}_3$ ,  $J = 6.8$  Hz); 1.26–1.35 (m, 22 H,  $\text{CH}_2\text{CH}_2(\text{CH}_2)_{11}\text{CH}_3$ ); 1.73–1.79 (m, 2 H,  $\text{CH}_2\text{CH}_2(\text{CH}_2)_{11}\text{CH}_3$ ); 3.28 (t, 6 H,  $\text{N}(\text{CH}_2\text{CH}_2)_3$ ,  $J = 7.5$  Hz); 3.51–3.55 (m, 2 H,  $\text{N}^+\text{CH}_2$ ); 3.69 (t, 6 H,  $\text{N}^+(\text{CH}_2\text{CH}_2)_3$ ,  $J = 7.6$  Hz). Found (%): C, 61.63; H, 10.61; Br, 20.54; N, 7.19.  $\text{C}_{20}\text{H}_{41}\text{BrN}_2$ . Calculated (%): C, 61.91; H, 10.86; Br, 20.46; N, 7.40.

**1-Hexadecyl-4-aza-1-azoniabicyclo[2.2.2]octane bromide (3).** The yield was 77%, m.p. 176–178 °C. IR (KBr),  $\nu/\text{cm}^{-1}$ : 2919, 2849, 1467, 1376, 1098, 1058, 850, 797, 720.  $^1\text{H}$  NMR ( $\text{CDCl}_3$ ),  $\delta$ : 0.87 (t, 3 H,  $\text{CH}_3$ ,  $J = 6.9$  Hz); 1.24–1.34 (m, 26 H,  $\text{CH}_2\text{CH}_2(\text{CH}_2)_{13}\text{CH}_3$ ); 1.73–1.75 (m, 2 H,  $\text{CH}_2\text{CH}_2(\text{CH}_2)_{13}\text{CH}_3$ ); 3.26 (t, 6 H,  $\text{N}(\text{CH}_2\text{CH}_2)_3$ ,  $J = 7.4$  Hz); 3.48–3.51 (m, 2 H,  $\text{N}^+\text{CH}_2$ ); 3.67 (t, 6 H,  $\text{N}^+(\text{CH}_2\text{CH}_2)_3$ ,  $J = 7.8$  Hz). Found (%): C, 63.23; H, 10.86; Br, 19.15; N, 6.71.  $\text{C}_{22}\text{H}_{45}\text{BrN}_2$ . Calculated (%): C, 63.29; H, 10.87; Br, 19.07; N, 6.42.

**1-Octadecyl-4-aza-1-azoniabicyclo[2.2.2]octane bromide (4).** The yield was 79%, m.p. 208–210 °C. IR (KBr),  $\nu/\text{cm}^{-1}$ : 2919, 2849, 1471, 1377, 1100, 1058, 850, 796, 720.  $^1\text{H}$  NMR ( $\text{CDCl}_3$ ),  $\delta$ : 0.88 (t, 3 H,  $\text{CH}_3$ ,  $J = 7.0$  Hz); 1.26–1.35 (m, 30 H,  $\text{CH}_2\text{CH}_2(\text{CH}_2)_{15}\text{CH}_3$ ); 1.72–1.78 (m, 2 H,  $\text{CH}_2\text{CH}_2(\text{CH}_2)_{15}\text{CH}_3$ ); 3.28 (t, 6 H,  $\text{N}(\text{CH}_2\text{CH}_2)_3$ ,  $J = 7.3$  Hz); 3.51–3.53 (m, 2 H,  $\text{N}^+\text{CH}_2$ ); 3.69 (t, 6 H,  $\text{N}^+(\text{CH}_2\text{CH}_2)_3$ ,  $J = 7.5$  Hz). Found (%): C, 64.70; H, 11.09; Br, 17.96; N, 6.29.  $\text{C}_{24}\text{H}_{49}\text{BrN}_2$ . Calculated (%): C, 64.30; H, 12.08; Br, 18.10; N, 6.13.

Surface tension was determined by the Du Nouy ring detachment method. Data on the specific electric conductance of solutions of compounds **1–4** were obtained on a CDM-2d instrument (Denmark). The concentration of the free bromide ion was determined with an I-160MI ionometer using an ELIS-131Br bromine-selective electrode. An ESR-10101 electrode was used as a reference.

Sizes of ensembles were determined on a PhotoCor Complex photon correlation spectrometer of dynamic and static light scattering and in the Malvern Zetasizer Nano system for characterization of nanoparticles (the angle of light scattering was 90° and 173°, respectively). A He–Ne gas laser with the wavelength 633 nm served as a laser radiation source.

ESR spectra were recorded at 22 °C on a Bruker Elexsys E500 X-range ESR spectrometer, the modulation frequency was 100 Hz, its amplitude was 0.3 G, and the microwave field power was 1.28 mW. The spin probe TEMPO (Sigma) was used. Glass capillaries with an inner diameter of 0.5 mm were used for measurements.

Viscosimetric measurements were carried out on an Ubbelohde viscosimeter using a temperature-controlled cell.

Bidistilled water was used for the preparation of all solutions studied.

## Results and Discussion

The tensiometric method of studying the properties of surfactant solutions is based on the measurement of a dependence of the surface tension ( $\gamma$ ) at the interface (liquid–gas, liquid–liquid, liquid–solid) vs the surfactant concentration. The dependences obtained for the surfactants belonging to the same homological series provide data that characterize the adsorption process of the compounds under study and their micelle formation properties and also allow one to consider a relationship of these phenomena and the surfactant structure. Figure 1, *a* shows the concentration plots of  $\gamma$  of solutions of compounds **1–4**. All studied compounds decrease  $\gamma$  to ~40  $\text{mN m}^{-1}$ , which is characteristic of solutions of the surfactants, whose surface tension does not exceed 30–50  $\text{mN m}^{-1}$  by absolute value.<sup>21</sup> In addition, the tensiometric dependences for compound **3** were studied in time (Fig. 1, *b*). The general run of the surface tension isotherms and the CMC values remain almost unchanged upon storage of the solution.

The maximum amount adsorbed ( $\Gamma_{\text{max}}$ ), minimum surface layer area per surfactant molecule ( $A_{\text{min}}$ ), standard free energy of adsorption ( $\Delta G_{\text{ad}}$ ), and free energy of micelle formation ( $\Delta G_{\text{m}}$ ) were calculated for the quantitative estimation of adsorption (Table 1). The following equations were used for the calculation:

$$\Gamma_{\text{max}} = -(2.3mRT)^{-1} \lim_{C \rightarrow \text{CMC}} (d\pi/d\log C),^{20} \quad (1)$$

where  $R$  is the universal gas constant,  $T$  is temperature,  $\pi$  is the surface tension equal to the difference between the surface tension values of the solvent and solution,  $m = 2$ , and  $C$  is the concentration of AD;

$$A_{\text{min}} = 10^{18}/(N\Gamma_{\text{max}}),^{24} \quad (2)$$

where  $N$  is Avogadro's number;

**Table 1.** Maximum amount adsorbed ( $\Gamma_{\text{max}}$ ), minimum surface layer area per surfactant molecule ( $A_{\text{min}}$ ), standard free energy of adsorption ( $\Delta G_{\text{ad}}$ ), and free energy of micelle formation ( $\Delta G_{\text{m}}$ ) of the cationic surfactants at 25 °C

Surfactant	$\Gamma_{\text{max}} \cdot 10^6$ /mol $\text{m}^{-2}$	$A_{\text{min}}$ /nm <sup>2</sup>	$-\Delta G_{\text{ad}}$ $-\Delta G_{\text{m}}$	
			kJ mol <sup>-1</sup>	
<b>1</b>	2.69	0.62	32.1	22.2
<b>2</b>	2.46	0.68	37.4	26.8
<b>3</b>	2.37	0.70	46.6	34.1
<b>4</b>	2.12	0.79	53.1	41.3
CPC <sup>a</sup>	2.34	0.71	41.2	28.2
CTAB <sup>b</sup>	3.10	0.53	37.5	30.6

<sup>a</sup> Literature data.<sup>22</sup>

<sup>b</sup> Literature data.<sup>23</sup>

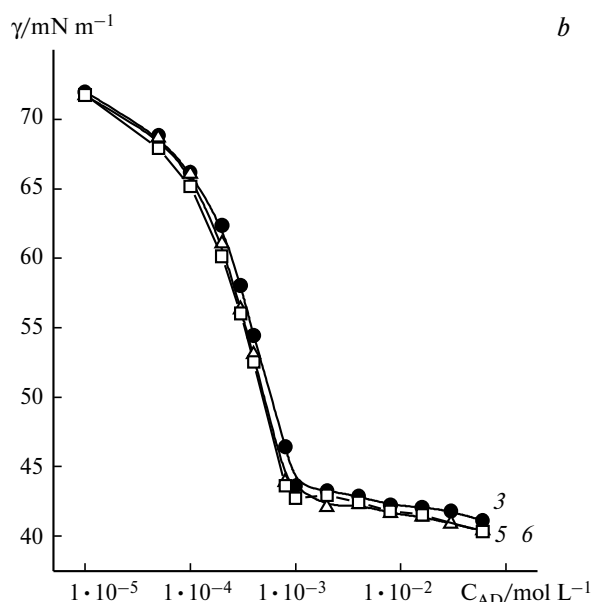
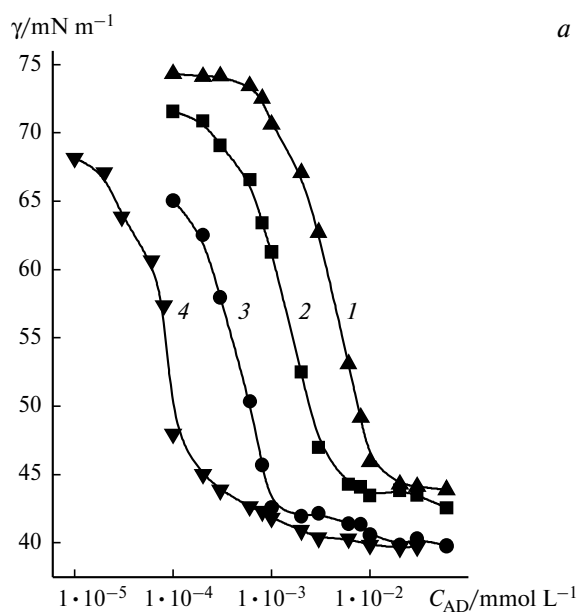


**Fig. 1.** Surface tension isotherms of aqueous solutions of **1** (I), **2** (2), **3** (3, 5, 6), and **4** (4) at 25 °C obtained during 1 (I–4), 3 (5), and 8 (6) days after preparation.

$$\Delta G_{\text{ad}} = \Delta G_{\text{m}} - (\pi_{\text{CMC}}/\Gamma_{\text{max}}),^{24,25} \quad (3)$$

$$\Delta G_{\text{m}} = (1 + g)RT \ln(\text{CMC}),^{24,25} \quad (4)$$

where  $g$  is the degree of binding of counterions.<sup>26</sup>

The CMC values corresponding to the inflections in the curves  $\gamma = f(C_{\text{AD}})$  (see Fig. 1) are listed in Table 2.

An increase in the hydrophobicity of the surfactant decreases weakly the maximum adsorption of the surfactant and increases  $A_{\text{min}}$  (see Table 1). It is known that during the adsorption of surfactant molecules at the interface the hydrophilic polar groups remain in the aqueous

*a*

**Table 2.** The CMC values of the cationic surfactants in water at 25 °C

Surfactant	CMC · 10 <sup>3</sup> /mol L <sup>−1</sup>		
	Tensio- metry	Conducto- metry	Potential- metry
<b>1</b>	11	14	16
<b>2</b>	4.0	3.0	3.7
<b>3</b>	1.0	1.0; 11 <sup>a</sup>	1.9
<b>4</b>	0.12	0.11; 0.91 <sup>a</sup>	0.22
CPC	0.85 <sup>b</sup>	0.98 <sup>c</sup>	—
CTAB	0.8 <sup>c</sup>	0.90 <sup>c</sup>	—

<sup>a</sup> The value of CMC<sub>2</sub>.

<sup>b</sup> Literature data.<sup>27</sup>

<sup>c</sup> Literature data.<sup>22</sup>

phase and the hydrophobic hydrocarbon chains are repulsed from it to the second phase. An increase in the surface area of the transversal cross section of the surfactant indicate a smaller density if the surface layer at the interface water–air interface, which agrees with the lower CMC values of the most hydrophobic homologs. At the same time, the elongation of the hydrocarbon radical of the bicyclic surfactant results in a decrease in the energy characteristics of the studied processes  $\Delta G_{\text{ad}}$  and  $\Delta G_{\text{m}}$ , *i.e.*, in a stronger decrease in the free energy of the system due to adsorption and micelle formation and an easier occurrence of these processes. According to Eq. (4), this should correlate with a decrease in the concentration at which micelles are formed. The latter tendency is also confirmed by the dependence of  $\log \text{CMC}$  on the number of carbon atoms ( $n$ ) in the hydrocarbon radical of the bicycle

$$-\log \text{CMC} = a + bn, \quad (5)$$

where  $a$  and  $b$  are the constants given in Table 3.

Note that for bicyclic surfactant **3** all parameters presented in Table 1 and the CMC value (see Table 2) are close to those for cetylpyridinium chloride (CPC), *i.e.*, a surfactant with the heterocyclic head group, whereas the  $\Gamma_{\text{max}}$  value of the noncyclic surfactant cetyltrimethylammonium bromide (CTAB) are somewhat higher and  $A_{\text{min}}$  are lower than those for surfactant **3** and CPC, indicating

**Table 3.** Coefficients  $a$  and  $b$  in Eq. (5) determined by different methods

Method	$a$	$b$	$r^a$
Tensiometry	−2.05	0.324	0.9862
Conductometry	−2.27	0.340	0.9907
Potentiometry	−1.75	0.294	0.9800

<sup>a</sup>  $r$  is the correlation coefficient.

the denser packing of head groups of the noncyclic surfactant compared to the cyclic ones.

The conductometric method also indicates the aggregation of the AD under study. The concentration plots of the electroconductivity ( $\chi$ ) of aqueous solutions of AD exhibit distinct breaks in the region of initial concentrations (Fig. 2 *a, b*) caused by the appearance of surfactant ensembles and the corresponding CMC<sub>1</sub> (see Table 2). The pronounced dependence of the absolute value of electroconductivity on the hydrophobicity of the surfactant is observed in the studied concentration range. The decrease in the electroconductivity of solutions observed with a decrease in the CMC value is due to the fact that the main contribution to the change in  $\chi$  value is made by the monomeric form of the surfactant,<sup>20</sup> whose concentration is determined by the CMC value. It should also be mentioned that a weakly pronounced second inflection (CMC<sub>2</sub>) appears in the concentration plot presented in Fig. 2 for cetyl homolog **3** (see Fig. 2, *a*), whereas the pronounced inflection is observed for octadecyl homolog **4** (see Fig. 2, *b*). The inflections indicate the rearrangement of the structure of the ensembles. The CMC<sub>2</sub> value is

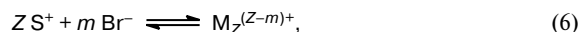
also affected by the alkyl substituted length. On going from **3** to **4**, the CMC<sub>2</sub> value decreases more than by an order of magnitude (see Table 2).

The potentiometric study using bromine-selective electrodes made it possible to determine the concentration of the free bromide ion, to estimate the critical micelle concentrations of AD, and to calculate the degree of binding of the counterions with AD micelles ( $\beta$ ) for the range of concentrations of the bicycles exceeding the CMC.

The CMC values correspond to the inflections in the concentrations dependences of  $[\text{Br}^-]$  (Fig. 3) and are given in Table 2.

The degree of binding of the counterions with AD micelles was calculated by the equation obtained from the consideration of the weight balance of the components of the system.

The equilibrium between the ions and counterions of the surfactants can be described by the equation



where  $Z$  is the average aggregation number;  $m$  is the average number of counterions bound to the micelle;  $\text{S}^+$  and  $\text{Br}^-$  are the surfactant ions and counterions, respectively;  $\text{M}_Z$  is the micelle with the aggregation number  $Z$ ;  $(Z - m)$  is the micelle charge.

The weight balance for the surfactant counterion and ion is described by the equations

$$C_{\text{tot}} = [\text{Br}^-] + m[\text{M}_Z], \quad (7)$$

$$C_{\text{tot}} = [\text{S}^+] + Z[\text{M}_Z], \quad (8)$$

where  $[\text{Br}^-]$  and  $[\text{S}^+]$  are the concentrations of free surfactant counterions and cations, respectively;  $[\text{M}_Z]$  is the concentration of micelles;  $C_{\text{tot}}$  is the total concentration of the surfactant.

Accepting that  $[\text{S}^+]$  is equal to the CMC, we have from Eq. (8) that the micelle concentration is expressed by the equation

$$[\text{M}_Z] = (C_{\text{tot}} - \text{CMC})/Z. \quad (9)$$

In this case, Eq. (7) can be written in the form

$$C_{\text{tot}} - [\text{Br}^-] = mZ^{-1}(C_{\text{tot}} - \text{CMC}). \quad (10)$$

The ratio  $mZ^{-1}$  expresses the degree of binding of counterions and, taking into account Eq. (10), is as follows:

$$\beta = (C_{\text{tot}} - [\text{Br}^-])/(C_{\text{tot}} - \text{CMC}). \quad (11)$$

The  $\beta$  values calculated by Eq. (11) are given in Fig. 3. An increase in the AD content insignificantly changes this parameter, and in the region of studied concentrations of **1**, **2**, and **4** the  $\beta$  values range from 0.67 to 0.84, whereas for compound **3** they lie in a range of 0.81–0.91.

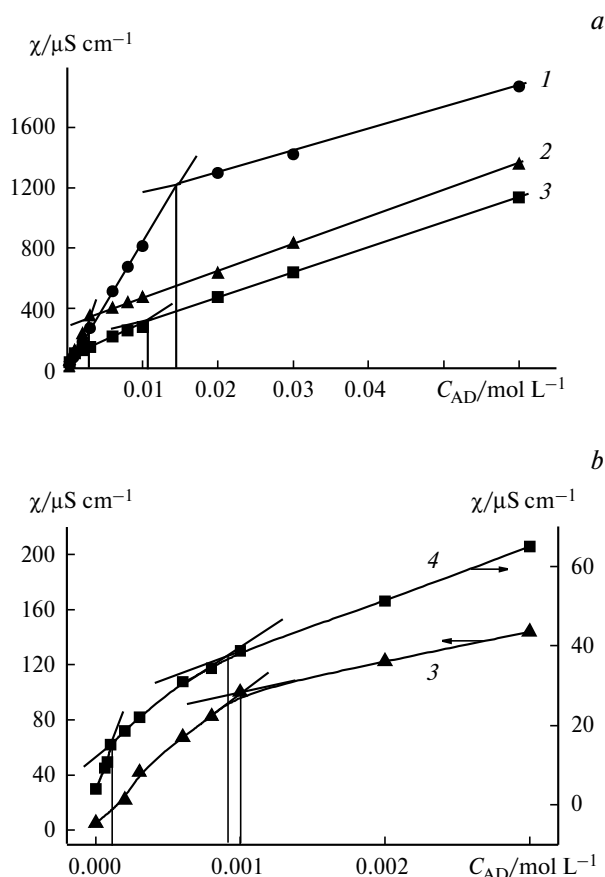


**Fig. 2.** Specific electric conductivity ( $\chi$ ) of aqueous solutions of **1** (**1**), **2** (**2**), **3** (**3**), and **4** (**4**) vs concentration at 25 °C in the region of initial concentrations:  $C_{\text{AD}} = 0\text{--}0.06$  (*a*) and  $0\text{--}0.003$  (*b*).

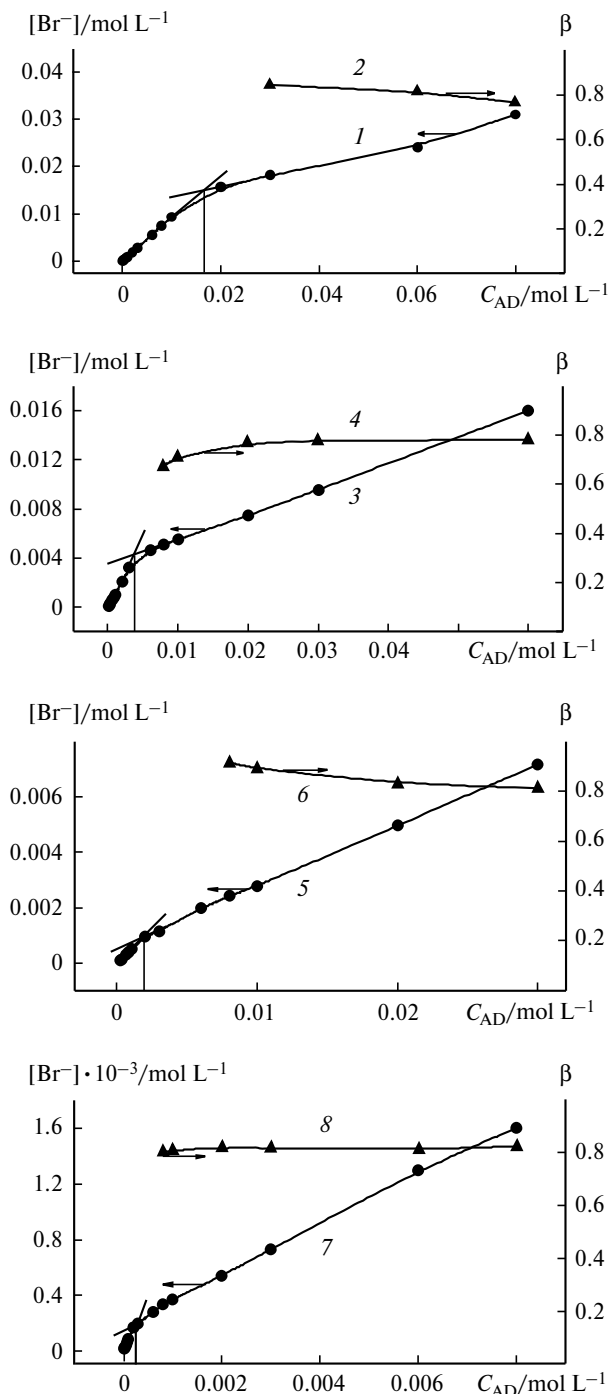


**Fig. 3.** Concentration of the free bromide ion (1, 3, 5, 7) and the degree of binding of the bromide ion with micelles (2, 4, 6, 8) in aqueous solutions of **1** (1, 2), **2** (3, 4), **3** (5, 6), and **4** (7, 8) vs AD concentration at 25 °C.

The use of the dynamic light scattering method makes it possible to determine the sizes of ensembles. As a rule, the hydrodynamic radius ( $R_{\text{eff}}$ ) of micelles of the typical surfactants near the CMC does not exceed 2–4 nm, which is below the sensitivity threshold of the method. Indeed,

we failed to measure the size of the ensembles for solutions of **1** and **2**. For longer-chain homologs **3** and **4**, after storage for several days, reproducible results were obtained, indicating that the solution contains large aggregates, whose size depends on the surfactant concentration (Fig. 4 *a, b*). For AD **4** the effective radii of the ensembles range from 90 to 140 nm and are independent from the storage time of the solutions (see Fig. 4, *b*). In the case of AD **3**, the size of the ensembles changes in time (see Fig. 4, *a*). The solutions are stabilized within 1–2 days; the ultrasonic treatment favors the formation of mono-dispersed systems. At the concentration of **3** equal to  $1 \cdot 10^{-3} \text{ mol L}^{-1}$ , *i.e.*, in the  $\text{CMC}_1$  region (see Table 2), the micelles are enlarged to the greatest extent upon the storage of the solution. In this case, the maximum value of the radius of the ensembles ( $R_{\text{max}}$ ) reaches 165 nm. An increase in the surfactant concentration is accompanied by a decrease in this parameter. For example, at the concentration of **3** equal to  $4 \cdot 10^{-3} \text{ mol L}^{-1}$  the  $R_{\text{max}}$  value is 90 nm, while in the region of  $\text{CMC}_2$  ( $C_3 = 10^{-2} \text{ mol L}^{-1}$ )  $R_{\text{max}} = 67 \text{ nm}$ . The example of the particle size distribution showed the absence of small ensembles corresponding to spherical micelles (Fig. 5).

Taking into account specificity of an aqueous solution of **3**, we carried out additional experimental studies by

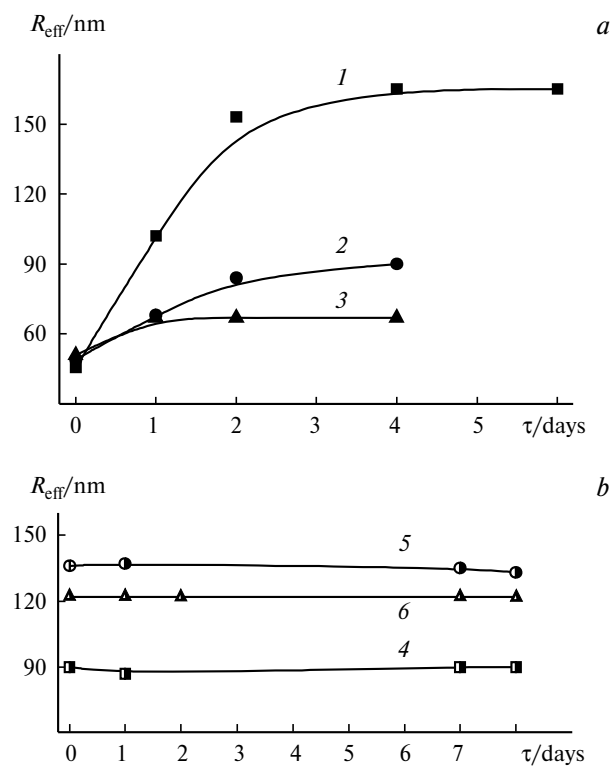


**Fig. 4.** Radius of ensembles of **3** (*a*, 1–3) and **4** (*b*, 4–6) in water vs time of staying of the solutions at 25 °C ( $C_{AD} = 1 \cdot 10^{-3}$  (1),  $4 \cdot 10^{-3}$  (2),  $1 \cdot 10^{-2}$  (3),  $2 \cdot 10^{-4}$  (4),  $6 \cdot 10^{-4}$  (5), and  $2 \cdot 10^{-3} \text{ mol L}^{-1}$  (6)).

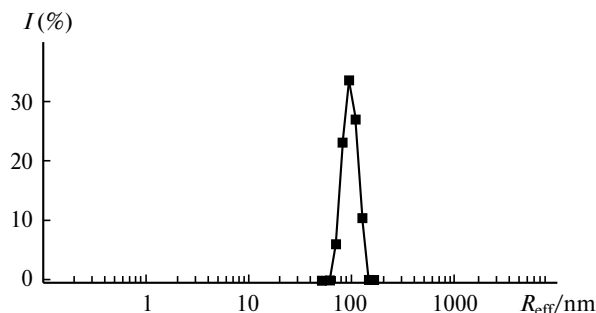


**Fig. 5.** Analysis of the size distribution of particles of **3** using the intensity parameter ( $C_{AD} = 1 \cdot 10^3 \text{ mol L}^{-1}$ ,  $25^\circ\text{C}$ , duration of staying of the solutions 1 day).

ESR spectroscopy and viscosimetry. The use of spin probes (mainly nitroxyl radicals) makes it possible to study the aggregation of surfactants in solutions and the dynamics of the process by ESR.<sup>28</sup> If a molecule with the attached radical rotates freely and isotropically, the spectrum consists of three lines of equal intensity and width. When the rotation of the probe is hindered, in particular, by the interaction with molecules of the environment, the width and intensity will change. These processes correspond to the correlation time from 0.01 to 10 ns. The rotation rate of the nitroxyl radical in this range is characterized by the correlation time  $\tau_c$  (see Ref. 29)

$$\tau_c = 6.5 \cdot 10^{-10} W_0 \left( \sqrt{\frac{h_0}{h_{-1}}} + \sqrt{\frac{h_0}{h_{+1}}} - 2 \right),$$

where  $W_0$  is the width of the central line;  $h_0$ ,  $h_{+1}$ , and  $h_{-1}$  is the height from the peak to the peak of the central, low-field, and high-field lines, respectively.

The change in the ESR spectrum upon the solubilization of the probe in micelles allows one to control such important characteristics of the ensembles as micropolarity, microviscosity, and packing density of molecules in the zone of localization of the radical probe. Therefore, the use of spin probes with different hydrophilic–lipophilic balances makes it possible to scan the microenvironment of the ensembles remote at different distances from the interfacial surface. Since we aimed at establishing structural rearrangements of the ensembles, which are most easily identified by the change in the compactness of surfactant molecules near the micellar surface (the so-called "palisade" layer), 2,2,6,6-tetramethyl-4-piperidine-*N*-oxyl (TEMPO) was used as a probe. According to the literature data<sup>30</sup> and the character of the ESR spectra, TEMPO is localized at the small depth of immersion into the micelle core, which agrees with the correlation times of the probe  $\leq 400 \text{ ps}$ . The results of calculation of the correlation time of the spin probe with an increase in the concentration of **3** are shown in Fig. 6. Two regions of sharp change in the parameter can be distinguished:

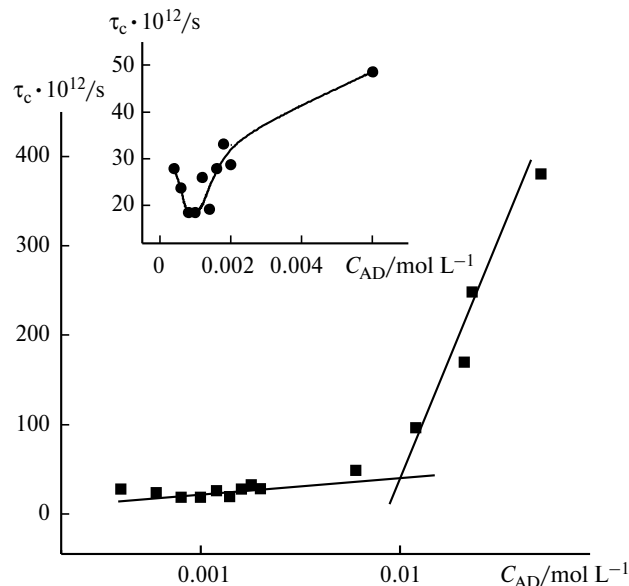


**Fig. 6.** Correlation time of the probe vs concentration of **3** ( $C_{\text{TEMPO}} = 5 \cdot 10^{-4} \text{ mol L}^{-1}$ ,  $22^\circ\text{C}$ ).

at a concentration of  $\sim 1 \cdot 10^{-3} \text{ mol L}^{-1}$  (inset) coinciding with the  $\text{CMC}_1$  and of  $\sim 0.01 \text{ mol L}^{-1}$  that coincides with the  $\text{CMC}_2$ . The sharp increase in the correlation time at the concentration  $> 0.01 \text{ mol L}^{-1}$  indicates the structural rearrangement in the system accompanied by the formation of ensembles with a more compact molecule packing.

The plots of the relative viscosity of solutions of **3** vs surfactant concentration are shown in Fig. 7. In the region of concentrations close to the  $\text{CMC}_1$ , an increase in the surfactant content in the solution exerts almost no effect on the relative viscosity value ( $\eta_{\text{rel}}$ ), but in the concentration region from 0.006 to 0.008  $\text{mol L}^{-1}$ , *i.e.*, approaching

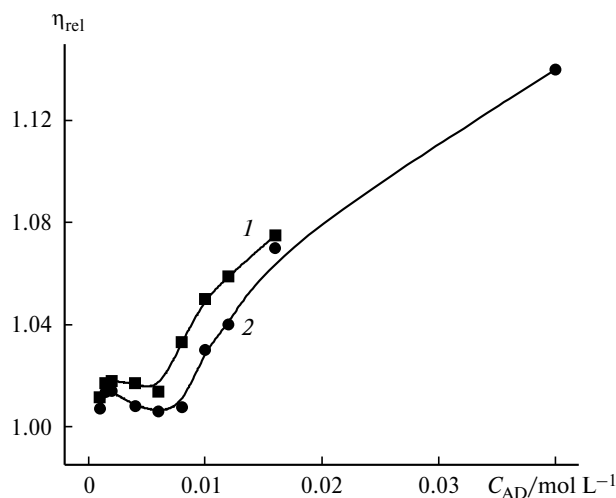


**Fig. 7.** Relative viscosity of freshly prepared (1) and stored for 3 days (2) aqueous solutions of **3** at  $25^\circ\text{C}$ .

the  $CMC_2$ , the  $\eta_{rel}$  values increase, indicating a change in the colloidal state of the solution. Thus, the transition to ensembles with a more compact packing of surfactant molecules was established for the system based on **3** at the  $CMC_2$  concentration.

Assuming that elongated micelles are present in the solution, we can calculate the ratio of semi-axes ( $P$ ) of the ensembles by the equation<sup>31</sup>

$$v = 2.5 + 0.4075(P - 1)^{1.508}. \quad (12)$$

In Eq. (12) the shape factor ( $v$ ) is related to the relative viscosity through the equation<sup>32</sup>

$$\eta_{rel} = 1 + v\phi + 14.1\phi^2, \quad (13)$$

where  $\phi$  is the volume fraction of the surfactant in the solution determined by the correlation

$$\phi = C_m \rho_0^{-1} (1 - d\rho/dC_m),$$

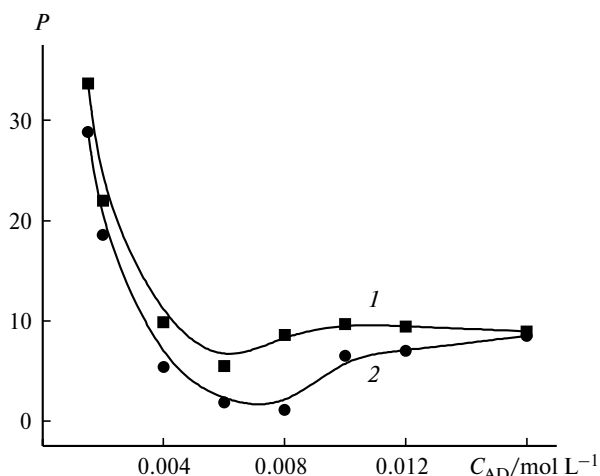
where  $C_m$  is the surfactant concentration in micelles ( $\text{g cm}^{-3}$ );  $\rho$  and  $\rho_0$  are the densities of the solution and solvent, respectively.

Figure 8 shows the concentration plots of the  $P$  parameter, which is  $> 1$  for all surfactant concentrations. In the case of both freshly prepared and stored for 3 days solutions of the bicyclic surfactant, beginning from a concentration of  $0.0015 \text{ mol L}^{-1}$ , an increase in the content of **3** decreases the  $P$  values. The minimum values of this parameter are achieved in the concentration region from  $0.006$  to  $0.008 \text{ mol L}^{-1}$ , the  $P$  values increase when the  $CMC_2$  is achieved ( $0.01 \text{ mol L}^{-1}$ ), and this parameter is stabilized with the further increase in the surfactant content in the solution. The most substantial decrease in the  $P$  parameter is observed in the region of low surfactant concentrations (down to 29 times), while  $P$  increases when

the  $CMC_2$  is achieved (by 8.5 times) for stored solutions of **3**. For the freshly prepared solutions in the region of low concentrations, the  $P$  parameter increases sixfold, whereas it increases by 1.8 times after the  $CMC_2$  is achieved. A comparison of these data with the sizes of the ensembles (see Fig. 4, a) indicates that the longest ensembles, which are transformed into more symmetric and compact (smaller in size) structures when the  $CMC_2$  is achieved, are formed in the case of the stored solutions in the region of the  $CMC_1$ . For the freshly prepared solutions, the transition of the strongly elongated to more symmetric structures occurs within almost one size of the ensembles. It can be assumed that the transition from micellar ensembles to vesicles occurs at concentrations in the  $CMC_2$  region. In this case, the whole array of results obtained for compound AD **3**, namely, an increase in the packing density of surfactant molecules and a large size remained unchanged at the low degree of symmetry of the ensembles, can be explained most satisfactorily.

The data obtained indicate that alkylated 1,4-diazabicyclo[2.2.2]octanes are surfactants capable of forming micelles in an aqueous medium. The elongation of the hydrocarbon AD radical decreases the standard free energy of adsorption at the water–air interface and also favors micelle formation in the solution. For the hexadecyl and octadecyl derivatives, the sizes of the ensembles formed depend on the concentration of the bicycle, whereas for compound **3** they also depend on the storage time of the solution. The largest ensembles of **3** are formed in the case of stored solutions in the region of critical micelle concentration, which can be due to the formation of the most elongated structures.

This work was financially supported by the Russian Foundation for Basic Research (Project Nos 09-03-00572-a and 09-03-12260-ofi\_m).



**Fig. 8.** Ratio of semi-axes of micellar ensembles ( $P$ ) formed in freshly prepared (1) and stored for 3 days (2) aqueous solutions of **3** vs surfactant concentration at  $25^\circ\text{C}$ .

## References

1. K. E. Price, S. J. Broadwater, H. M. Jung, D. T. McQuade, *Org. Lett.*, 2005, **7**, 147.
2. J. H. Li, J. L. Li, D. P. Wang, S. F. Pi, Y. X. Xie, M. B. Zhang, X. C. Hu, *J. Org. Chem.*, 2007, **72**, 2053.
3. J. W. Baker, J. B. Holdsworth, *J. Chem. Soc.*, 1947, 713.
4. J. C. Philips, Y. V. Swisher, D. Haidukewich, O. Morales, *Chem. Commun.*, 1971, 22.
5. R. S. Ray, R. B. Misra, M. Farooq, R. K. Hans, *Toxicol in vitro*, 2002, **16**, 123.
6. K. Nakagawa, K. Tajima, *Langmuir*, 1998, **14**, 6409.
7. H. Gerner, D. Dopp, *J. Chem. Soc., Perkin Trans. 2*, 2002, 120.
8. V. R. Verlan, *Tetrahedron Lett.*, 1969, **10**, 985.
9. H. Mansikkamaki, M. Nissinen, K. Rissanen, *Chem. Commun.*, 2002, 1902.
10. H. Mansikkamaki, M. Nissinen, C. A. Schalley, K. Rissanen, *N. J. Chem.*, 2003, **26**, 88.
11. L. Baldini, P. Ballester, A. Casnati, R. M. Gomila, C. A. Hunter, F. Sansone, R. Ungaro, *J. Am. Chem. Soc.*, 2003, **125**, 14181.

12. R. C. Doss, W. B. Reynolds, USA Pat. 3018619; *Chem. Abstrs.*, 1962, **56**, 15719.
13. W. E. Erner, USA Pat., 3073827; *Chem. Abstrs.*, 1963, **59**, 643.
14. F. M. Menger, R. A. Persichetti, *J. Org. Chem.*, 1987, **52**, 3451.
15. A. R. Katritzky, M. S. C. Rao, J. Stevens, *J. Heterocycl. Chem.*, 1991, **28**, 1115.
16. I. Tabushi, J. J. Imuta, N. Seko, Y. Kobuke, *J. Am. Chem. Soc.*, 1978, **100**, 6287.
17. O. Hromatka, O. Kraupp, *Monatsh. Chem.*, 1951, **82**, 880.
18. A. Vecchi, B. Melai, A. Marra, C. Chiappe, A. Dondoni, *J. Org. Chem.*, 2008, **73**, 6437.
19. N. V. Tamkovich, A. V. Malyshev, D. A. Konevets, V. N. Sil'nikov, M. A. Zenkova, V. V. Vlasov, *Bioorg. Khim.*, 2007, **33**, 251 [*Russ. J. Bioorg. Chem. (Engl. Transl.)*, 2007, **33**].
20. K. Shinoda, T. Nakagawa, B. Tamamushi, T. Isemura, *Colloidal Surfactants*, Academic Press, New York—London, 1963.
21. E. D. Shchukin, A. V. Pertsev, E. A. Amelina, *Kolloidnaya Khimiya [Colloid Chemistry]*, Vysshaya Shkola, Moscow, 2004, 445 pp. (in Russian).
22. S. P. Moulik, M. E. Haque, P. K. Jana, A. R. Das, *J. Phys. Chem.*, 1996, **100**, 701.
23. F. G. Valeeva, A. V. Zakharov, M. A. Voronin, L. Ya. Zakharova, L. A. Kudryavtseva, O. G. Isaikina, A. A. Kalinin, V. A. Mamedov, *Izv. Akad. Nauk, Ser. Khim.*, 2004, 1504 [*Russ. Chem. Bull. (Engl. Transl.)*, 2004, 1563].
24. S. Ghosh, *J. Colloid Interface Sci.*, 2001, **244**, 128.
25. S. Ghosh, S. P. Moulik, *J. Colloid Interface Sci.*, 1998, **208**, 357.
26. A. I. Rusanov, V. B. Fainerman, *Dokl. Akad. Nauk USSR*, 1989, **308**, 651 [*Dokl. Chem. (Engl. Transl.)*, 1989, **308**].
27. C. C. Addison, C. G. L. Furnidge, *J. Chem. Soc.*, 1956, 3229.
28. A. M. Vasserman, *Usp. Khim.*, 1994, **63**, 391 [*Russ. Chem. Rev. (Engl. Transl.)*, 1994, **63**, 373].
29. D. Kivelson, *J. Chem. Phys.*, 1960, **33**, 1094.
30. S. Vziayan, C. Kamachandran, D. R. Woods, *Can. J. Chem. Eng.*, 1980, **58**, 485.
31. A. I. Serdyuk, R. V. Kucher, *Mitsellyarnye perekhody v rastvorakh poverkhnostno-aktivnykh veshchestv [Micellar Transitions in Solutions of Surfactants]*, Naukova Dumka, Kiev, 1987, 208 pp. (in Russian).
32. A. I. Serdyuk, I. L. Povkh, V. I. Podmarkov, *Zh. Prikl. Khim.*, 1982, **55**, 1044 [*J. Appl. Chem. USSR (Engl. Transl.)*, 1982].

Received May 5, 2009;  
in revised form May 7, 2010